Analysis of a model for resonant extraction of intense beams by normal forms and frequency map

L. Bongini, A. Bazzani, and G. Turchetti
Dipartimento di Fisica, Via Irnerio 46, 40126 Bologna, Italy

I. Hofmann
GSI, Planckstrasse 1, D-64291 Darmstadt, Germany

(Received 19 October 2000; revised manuscript received 26 June 2001; published 28 November 2001)

A simple 1D model is proposed to explore the resonant extraction of intense beams from a synchrotron as performed in the SIS synchrotron in GSI (Darmstadt). The model Hamiltonian consists of a constant focusing, a thin sextupole, and a smooth space charge field. Hyperbolic normal forms are used to estimate the extraction times and the emittance of the extracted beam; the quality of the reconstruction is tested in absence of space charge. The effect of space charge on the dynamical behavior of the beam near the $1/3$ betatron resonance is numerically investigated using the frequency map analysis and qualitatively explained with perturbation theory. A polynomial approximation to the one turn map is obtained by replacing the exact space charge force with a sequence of polynomial kicks, and the resonant normal forms reproduce quite accurately the nonlinear tunes and the fixed points position. At low order an analytical estimate of the area of the stable region is proposed to recover the self-consistency of the model.

DOI: 10.1103/PhysRevSTAB.4.114201 PACS numbers: 29.20.Hm, 29.27.Ac, 52.40.Mj, 11.10.Ef

I. INTRODUCTION

In the study of rare nuclear reactions by means of beam-target collision experiments, the intensity of the delivered beam is often limited by some overheating constraints (the target may melt). One needs then to dilute the extraction on a time interval depending on external requirements. The tool traditionally used for this purpose is resonant (or slow) extraction. By means of nonlinear magnetic elements (usually sextupoles or octupoles) one excites an unstable resonance that divides the transverse phase space (usually the horizontal one) into a stable and an unstable region. Particles are then gradually destabilized by shrinking the dimensions of the stable area (which can be done by either quadrupole ramping or betatron core acceleration) or by making them diffuse outside by means of a an rf noise applied perpendicularly to the beam.

In the study of rare reactions, however, the beam intensities needed at the target could be so high that the current circulating in the beam is sufficient to produce significant space charge effects. A 500 mA beam of U^{72+}, as planned at the SIS synchrotron in GSI (Darmstadt), causes, for example, a relative linear tune shift of 5×10^{-3}. In this case the space charge effects on the resonant extraction should be considered because a slow spill is required not to melt the target.

The purpose of this paper is to illustrate a method, based on the normal forms perturbative technique, to give semianalytical estimates for the extraction times and emittances of the extracted beam. These two parameters are of basic importance to understand the influence of ripples, present in the power supplies, on the temporal density profile of the extracted beam and on the focal spot. The advantage of semianalytical estimates with respect to tracking procedures lies in an easier parametric control of the extraction mechanism. These estimates, given for a fixed machine tune, can be used also in the case of quadrupole ramping and betatron core acceleration, provided that they are performed slowly enough to be considered adiabatic processes (spills longer than 10 ms for machine circumferences of some hundreds of meters).

The method is based on the computation of the fixed hyperbolic points of the accelerator one turn map and on the calculation, in their neighborhood, of the hyperbolic normal form. After a nonlinear transformation to normal coordinates, the map becomes hyperbolic with a divergence factor which depends on the invariant, so that the computation of the extraction time and extracted emittance becomes very easy. When no resonance islands are present, the validity domain of these perturbative estimates can be indefinitely extended along the stable and unstable manifolds, otherwise the island elliptic fixed point determines a border.

The proposed technique is first applied to the study of a case without space charge. The estimate obtained for the extraction time is comparable, at the lowest order, with the result of a previously proposed method for extraction through the $1/3$ resonance [1], while at higher orders it allows one to take into account the strong nonlinear deformation of the unstable orbits, which considerably affects the extraction time behavior. Moreover, being free of *ad hoc* assumption on the dynamics, it allows an automatic extension to resonances different from $1/3$ and to nonlinear fields different from the pure sextupolar one.

In the presence of space charge the stable area changes and the hyperbolic fixed points move. A careful modeling

of the nonlinear influence of space charge on transversal resonances is then needed to locate the new fixed points and to extend the proposed technique to the study of an intense beam.

The outline of the paper is as follows. In Sec. II we specify the Hamiltonian describing a flat intense beam in a linear lattice with a thin extraction sextupole. In Sec. III we introduce the hyperbolic normal forms to analyze the dynamics of the one turn map and to compute the extraction times, when the linear tune is close to $1/3$ and the space charge is negligible. In Sec. IV we investigate the dynamical effects of the space charge by analyzing the changes induced in the tune and the dynamic aperture. A semianalytic estimate of the tune and of the stable area, provided by the resonant elliptic normal forms, allows one to impose an approximate self-consistency condition and to define an effective sextupolar strength.

II. PRESENTATION OF THE MODEL

The proposed model refers to the horizontal motion of a particle belonging to a round beam and moving in a linear lattice with a thin extraction sextupole and subject to the space charge force

$$F = -\frac{\xi}{2a} V'\left(\frac{x}{a}\right), \tag{1}$$

where ξ is the perveance of the beam, a its radial extension, and $V(x)$ is the electric potential for a unit charge per unit length and unit beam radius. We choose the potential

$$V(x) = -\log(1 + x^2) \tag{2}$$

corresponding to an electric field which behaves linearly at the origin and vanishes similar to $1/x$ as $x \to \infty$ The force acting on a macroparticle has the same asymptotic behavior as for a KV distribution but mimics a smooth distribution of charge at the core edge and reads

$$F = \frac{\xi}{a^2} \frac{x}{1 + \frac{x^2}{a^2}}. \tag{3}$$

The corresponding Hamiltonian in the physical coordinates is

$$H_{\rm ph} = \frac{p_{\rm ph}^2}{2} + k_0 \frac{x_{\rm ph}^2}{2} - \frac{K_2}{6} x_{\rm ph}^3 \delta_L(s_{\rm ph}) + \frac{\xi}{2} V\left(\frac{\xi_{\rm ph}}{a}\right), \tag{4}$$

where k_0 is the machine quadrupolar gradient, K_2 is the integrated sextupolar gradient, and $\delta_L(s)$ is the periodic δ function of period L, the length of the ring.

For $\xi = 0$, the betatronic frequency for particles with vanishingly small oscillation amplitude is $\omega_0 = \sqrt{k_0} L$. When $\xi \neq 0$ the quadratic term of V changes the frequency as $\omega^2 = \omega_0^2 - \xi L^2/a^2$ and the tune shift is $\Delta Q_{\rm sc} = (\omega_0 - \omega)/2\pi \simeq \xi L^2 a^{-2}/4\pi\omega_0$.

A. Scalings

Scaling the longitudinal and transverse coordinates according to $s = s_{\rm ph}/L$ and $x = x_{\rm ph}$, $p = p_{\rm ph} L$, we write the scaled Hamiltonian $H = L^2 H_{\rm ph}$ as a function of the depressed linear frequency ω,

$$H = \frac{p^2}{2} + \omega^2 \frac{x^2}{2} - \frac{K_2 L}{6} x^3 \delta(s) + \frac{\xi L^2}{2}\left[V\left(\frac{x}{a}\right) + \frac{x^2}{a^2}\right], \tag{5}$$

where $\delta_L(Ls) = L^{-1}\delta(s)$ and $\delta(s)$ has period 1. We notice that the scaled emittance is $\epsilon = L\epsilon_{\rm ph}$ and that Hamilton's equations still hold in the scaled variables. Moving then to the linearly normalized coordinates $\hat{x} = x\sqrt{\omega}$, $\hat{p} = p/\sqrt{\omega}$, the Hamiltonian reads

$$H = \omega \frac{\hat{x}^2 + \hat{p}^2}{2} - \frac{\hat{K}_2}{6} \hat{x}^3 \delta(s) + \frac{\hat{\xi}}{2} \hat{a}^2\left[V\left(\frac{\hat{x}}{\hat{a}}\right) + \frac{\hat{x}^2}{\hat{a}^2}\right], \tag{6}$$

where $\hat{a} = a\sqrt{\omega}$ is the normalized radius, and

$$\hat{K}_2 = \frac{L K_2}{\omega^{3/2}}, \qquad \hat{\xi} = \frac{\xi L^2}{\hat{a}^2} = \frac{\xi L^2}{a_\omega^2} \tag{7}$$

are the scaled sextupolar gradient and the scaled perveance. The Courant-Snyder–like coordinates $\hat{x}, \hat{p}$ have the dimension of a length similar to x, p, whereas $\hat{K}_2$ is the inverse of a length.

A dimensionless description is obtained after scaling Eq. (5) or (6) with respect to the core radius $x/a, p/a$, or $\hat{x}/a, \hat{p}/a$ and H/a^2; the emittance becomes ϵ/a^2. Using the normalized coordinates we have

$$\frac{H}{a^2} = \frac{\omega}{2}\left(\frac{\hat{p}^2}{a^2} + \frac{\hat{x}^2}{a^2}\right) + \frac{\hat{K}_2 a}{6} \frac{\hat{x}^3}{a^3} \delta(s) + \frac{\hat{\xi}}{2}\left[\omega V\left(\frac{\hat{x}}{a\sqrt{\omega}}\right) + \frac{\hat{x}^2}{a^2}\right],$$

and the Hamiltonian depends on the dimensionless parameters ω, $\hat{K}_2 a$, and $\hat{\xi}$

B. Dynamic aperture

For a real lattice in the extraction regime the bare linear tune is given by $Q_0 = m + \frac{1}{3} + \frac{\eta}{2\pi}$, where m is the integer part and $\eta \ll 1$. Letting $n = 3m + 1$ we have $\omega_0 = 2\pi\frac{n}{3} + \eta$. The dynamic aperture in the absence of space charge depends only on η,

$$\hat{x}_{\rm dyn} = \frac{2}{\hat{K}_2} D(\omega_0), \qquad x_{\rm dyn} = \frac{2\omega_0}{K_2 L} D(\omega_0). \tag{8}$$

$D(\omega_0) \sim 3|\eta|$ is the dynamic aperture of the Hénon map.

If we change ω_0 into $\omega_0' = \frac{2\pi}{3} + \eta$ by choosing a ring of length $L' = L/n$ and $k_0' = k_0(n\omega_0'/\omega_0)^2 \simeq k_0$, the

dynamic aperture $x_{\rm dyn}$, in physical coordinates is unchanged since $\omega_0' \simeq \omega_0/n$ implies $\omega_0/L \simeq \omega_0'/L'$.

The presence of space charge changes ω_0 into ω, but the tune depression does not vary since $\omega/\omega_0 = \omega'/\omega_0'$, whereas the tune shift changes by $1/n$ being proportional to the ring length. To have the same dynamic aperture, which depends on $\eta + \hat{\xi}/2 = \eta + \xi L^2/2a^2\omega$, the perveance for the short ring must be changed into $\xi' = n\xi$. Finally, the normalized parameters for long and short rings are related by

$$\hat{K}_2' = \frac{K_2 L'}{\omega'^{3/2}} = \sqrt{n}\,\hat{K}_2, \qquad \hat{\xi}' = \frac{n\xi L'^2}{\omega' a^2} = \hat{\xi}\,.$$

C. A realistic example

We quote the parameters of the SIS synchrotron at GSI for an extraction of 500 mA of U^{72+} at 1000 MeV per nucleon; the longitudinal and transverse length units are meters and millimeters. The ring length is $L \simeq 217$ m, the bare tune is $Q_0 = 4.3$ ($\langle\beta\rangle = 8$ m), and the sextupole gradient is $K_2 \simeq 3\ \mathrm{m}^{-2}$. The initial horizontal emittance is 200 mm mrad, the core radius is $a \simeq 25$ mm, and the tune shift is $\Delta Q_{\rm sc} \simeq 5 \times 10^{-3}$ (1000 times less for therapeutic applications) implying $\xi \simeq 0.02$. The normalized parameters are $\hat{K}_2 = 4.6\ \mathrm{m}^{-1}$, $\hat{\xi} \simeq 6 \times 10^{-2}$, and $\hat{a} = 130$ mm. In the models chosen for our simulations the values of the parameters $\hat{K}_2$ and $\hat{\xi}$ are comparable with SIS. This Hamiltonian is not self-consistent since the beam radius is a free parameter. A self-consistent radius $\hat{a}$ depends on ω_0, $\hat{K}_2$, $\hat{\xi}$ as shown in the previous section.

III. HYPERBOLIC INTERPOLATING HAMILTONIAN

In this section we show how to obtain semianalytical estimates of the extraction time and the emittance of the extracted beam in the case of a pure sextupole. The proposed method relies on the computation of the hyperbolic normal form. After calculating the one turn (Poincaré) map M, we chose one of the hyperbolic periodic points $(\hat{x}_f, \hat{p}_f)$ of period 3. This is a fixed point for the third iterate of the map $M^{\circ 3}$, $(\hat{x}_f, \hat{p}_f)$ and the orbits are close to hyperbolas in its neighborhood. After translating the origin to $(\hat{x}_f, \hat{p}_f)$, we look for an approximate symplectic change of coordinates $X(\hat{x}, \hat{p})$, $P(\hat{x}, \hat{p})$, such that in the new coordinates the motion generated by $M^{\circ 3}$ is exactly hyperbolic. This transformation is defined in a neighborhood of the unstable fixed point and can be extended along the stable and unstable manifolds [2]. The interpolating Hamiltonian $\mathcal{H}$ in the new coordinates $\mathcal{H} = H_0 + H_1 XP + H_2 (XP)^2 + \cdots$ is a power series in XP, and the invariant curves are equilateral hyperbolae. Letting $\sigma = \partial\mathcal{H}/\partial(XP)$ the evolution is given by

$$\begin{aligned} X(t) &= X_0 e^{\sigma(X_0P_0)t/3}, \\ P(t) &= P_0 e^{-\sigma(X_0P_0)t/3}, \end{aligned} \tag{9}$$

where $(X(3t), P(3t))$ interpolates the iterates of order of $M^{\circ 3}$ defined for t integer. The exponential divergence rate from the origin, σ, depends on the invariant XP, as the tune of a closed orbit depends on the emittance. If the initial point is near to the hyperbolic fixed point, the orbit spends a rather long time nearby, until $X(t)$ becomes of order 1, but the subsequent divergence is fast. Denoting by $X_{\rm es}$ the abscissa of the point where the image of the septum in the normal coordinates plane intersects the orbit with initial conditions (X_0, P_0), the extraction time $t_{\rm es} = 3T$ reads $X(t_{\rm es}) \equiv X(3T) = X_{\rm es}$.

The value of T is given by

$$T = \frac{1}{\sigma(X_0P_0)} \log\frac{X_{\rm es}}{X_0}\,. \tag{10}$$

We consider two cases corresponding to different conditions for the extraction process: (i) the particles are extracted near the unstable manifold issued from the hyperbolic point, and (ii) the particles escape through the stochastic layer surrounding a resonance island and are extracted. The first case is illustrated by the top frame of Fig. 1, the second by the top frame of Fig. 2. In the bottom frames of Figs. 1 and 2 we compare the extraction times computed from the hyperbolic normal forms of different orders with the results obtained from tracking. The extraction time computed from the lowest order normal form decreases monotonically with the distance from the hyperbolic point. The numerical simulation, on the contrary, shows that a minimum extraction time is achieved at some distance.

This behavior is explained by higher order normal forms as a folding effect of the trajectories, which two times crosses the segment where the initial conditions are chosen; see the bottom frame of Fig. 3. This effect is more visible in the normal coordinates space, where the trajectories are equilateral hyperbolas and the initial condition line has folded; see the top frame of Fig. 3. As a consequence, when we move along this line of initial points every trajectory is crossed two times. The intersection points A, B of a trajectory have different extraction times: if the point A is met first when we move along the line of initial conditions, the extraction time of B is the same as A plus the time needed to go from B to A along the trajectory joining them. In case (ii) the initial conditions set crosses the stable manifold, where the escape time diverges; see bottom frame of Fig. 2.

Beyond the stable manifold (vertical axis in the top frame of Fig. 3) the particle follows another family of hyperbolas. In the bottom frame of Fig. 3 we have plotted, in the x, p plane, the images of the stable and unstable manifolds, which cross at the first homoclinic point at a very small angle. This point is a singularity for the Taylor expansion of the normal form transformation and defines the applicability limit of the normal form dynamics.

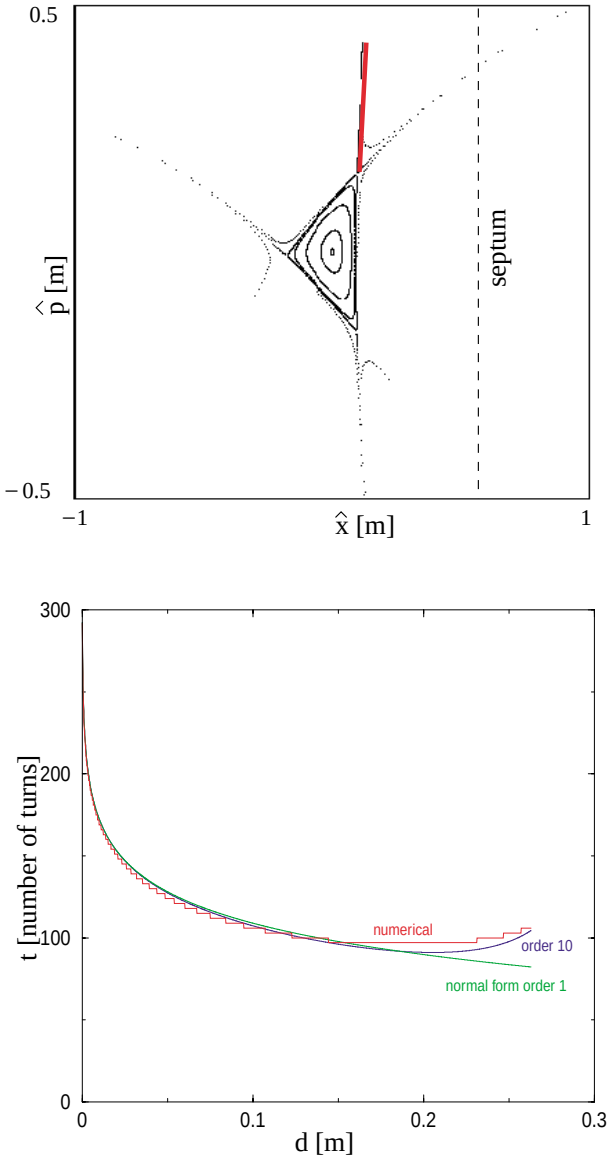

FIG. 1. (Color) (Top) Phase plot in linearly normalized coordinates $(\hat{x}, \hat{p})$ for a sextupole $\hat{K}_2 = 1\ \mathrm{m}^{-1}$ and linear frequency $\omega_0 = 4.33 \times 2\pi$. (Bottom) Numerical (red line) and analytical (blue, first order; green, tenth order) estimates of the extraction time for a distribution of particles on a line versus the distance from the hyperbolic fixed point. The extracted points initially belong to the red segment in the phase space plot. The dynamic aperture is $\hat{x}_{\mathrm{dyn}} = 90$ mm. The corresponding value in the physical coordinates is $x_{\mathrm{dyn}} = 17$ mm, and for the value $\hat{K}_2 = 4.6\ \mathrm{m}^{-1}$ of SIS becomes $x_{\mathrm{dyn}} \simeq 4$ mm.

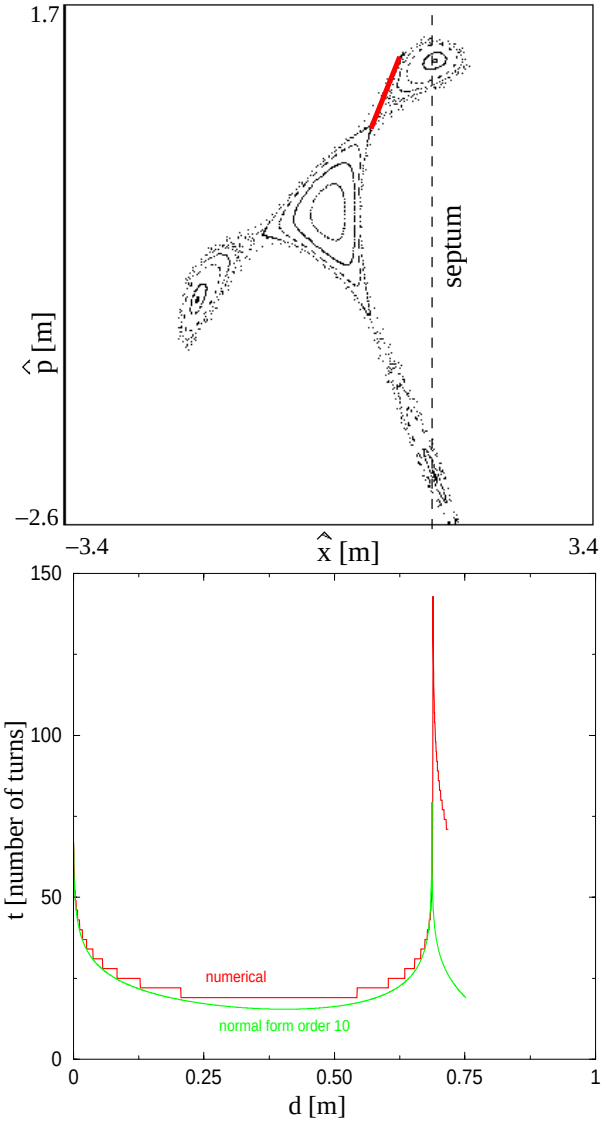

FIG. 2. (Color) (Top) Phase plot in linearly normalized coordinates $(\hat{x}, \hat{p})$ for a sextupole $\hat{K}_2 = 1\ \mathrm{m}^{-1}$ and linear frequency $\omega_0 = 4.32 \times 2\pi$. (Bottom) Numerical (red line) and analytical tenth-order (green) estimates of the extraction time for a distribution of particles on a line versus the distance from the hyperbolic fixed point. The extracted points initially belong to the red segment in the phase space plot. The dynamic aperture is $\hat{x}_{\mathrm{dyn}} = 570$ mm. The corresponding value in physical coordinates is $x_{\mathrm{dyn}} = 110$ mm, and for the value $\hat{K}_2 = 4.6\ \mathrm{m}^{-1}$ of SIS becomes $x_{\mathrm{dyn}} = 24$ mm, just as the core radius a at the beginning of the extraction.

Another straightforward calculation in normal coordinates is the extracted emittance ϵ. We consider the invariant curve to which belongs the initial point (X_0, P_0) such that $X_{\mathrm{es}} = X(3T) = X_0 e^{T\sigma(X_0P_0)}$. The areas $\pi\epsilon_k$ of the domains D_k delimited by the horizontal axis $P = 0$, the curve $XP = X_0P_0$, and the vertical lines $X = X(3k-3)$, $X = X(3k)$ for $k = 1, \ldots, T$ (see Fig. 4) are all equal and are given by

$$\pi\epsilon_k = \int_{X(3k-3)}^{X(3k)} P(X)dX = X_0P_0 \log\left(\frac{X(3k)}{X(3k-3)}\right) = X_0P_0\sigma(X_0P_0)\,. \quad (11)$$

The domains $D_1, D_2, \ldots, D_T$ are extracted at time $3T, 3T-3, \ldots, 3$, respectively.

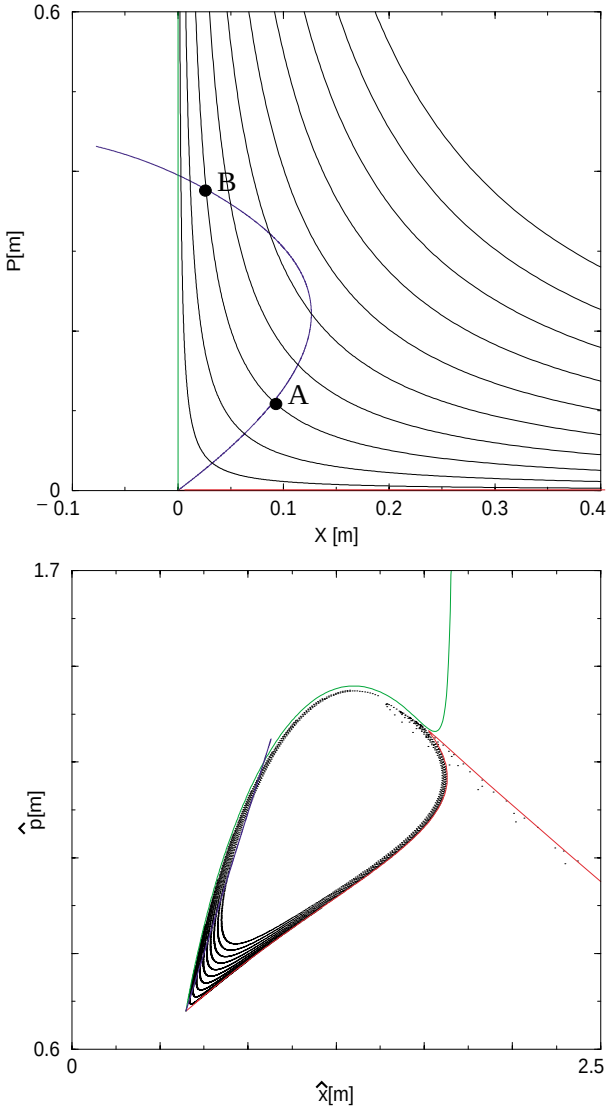

FIG. 3. (Color) (Bottom) Magnification of the top of Fig. 2 with the segment (blue) on which the initial conditions are chosen, the unstable (red) and stable (green) manifolds. (Top) Image in normal coordinates (X, P) of a neighborhood of the hyperbolic point, the initial conditions segment (blue curve), and the stable (P axis) and unstable (X axis) manifolds.

If the curve bounding the domains D_k is not an invariant curve, the extracted areas $\pi\epsilon_k$ are no longer constant and typically the emittance ϵ_k extracted at time $t = 3(T - k + 1)$ is an increasing function of k; see Fig. 6. Therefore the emittance ϵ is a decreasing function of t. To this end we consider a rectangular region partitioned into rectangular domains $D_1, D_2, \ldots, D_T$ where the hyperbola to which (X_0, P_0) belongs is replaced by the straight line $P = P_0$ (see Fig. 5). We can easily show that $\epsilon_1 < \epsilon_2 < \cdots < \epsilon_T$, as observed in a numerical simulation (where the domain is rectangular in the initial coordinates) whose results are shown in Fig. 6. Indeed D_T is split by the hyperbola passing through $(X(3T - 3), P_0)$

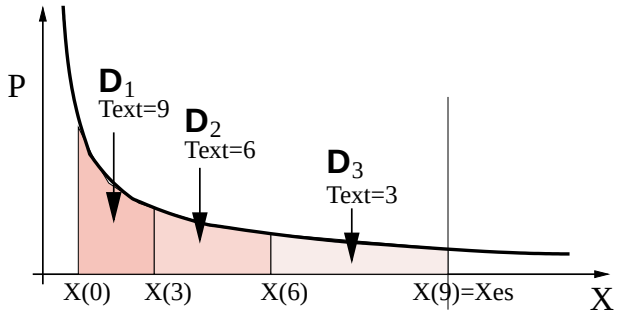

FIG. 4. (Color) Calculation in the normal coordinates frame of the emittance of the extracted beam. The points in the lightest domain D_3 are extracted after three iterations of the map M, and its area is the emittance extracted in that period. The points in the domains D_2, D_1 are extracted after six and nine iterations, respectively.

into two domains: U_T (upper) and L_T (lower). The same hyperbola and the straight lines $X = X(3T - 6)$, $X = X(3T - 3)$, $P = 0$ define a domain which is the union D_{T-1} and a nonempty domain A_{T-1} (see Fig. 5) where $M^{\circ 3}(D_{T-1} \cup A_{T-1}) = L_T$. As a consequence,

$$\begin{aligned} \pi\epsilon_T &= \text{area}(D_T) = \text{area}(L_T) + \text{area}(U_T) \\ &= \text{area}(D_{T-1}) + \text{area}(A_{T-1}) + \text{area}(U_T) \\ &= \pi\epsilon_{T-1} + \mu\,, \end{aligned} \tag{12}$$

where $\mu = \text{area}(A_{T-1}) + \text{area}(U_T)$ is strictly positive since the domains are nonempty. The above estimates can be used in two distinct ways.

(i) Static case.—The effect on the extracted emittance of the ripples present in the power supplies can be analyzed. In the presence of ripples the boundary of the stable region moves inward and outward periodically. The particles swept in one period are immediately destabilized. The amplitude of this layer depends on the amplitude stable region. Computing $\epsilon(XP)$ and $T(XP)$ on its

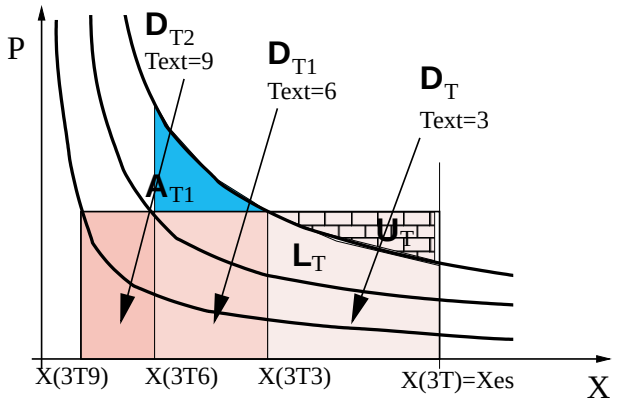

FIG. 5. (Color) Sketch, in the normal coordinates frame, of the extracted emittance for a rectangular set of initial conditions and $T = 3$.

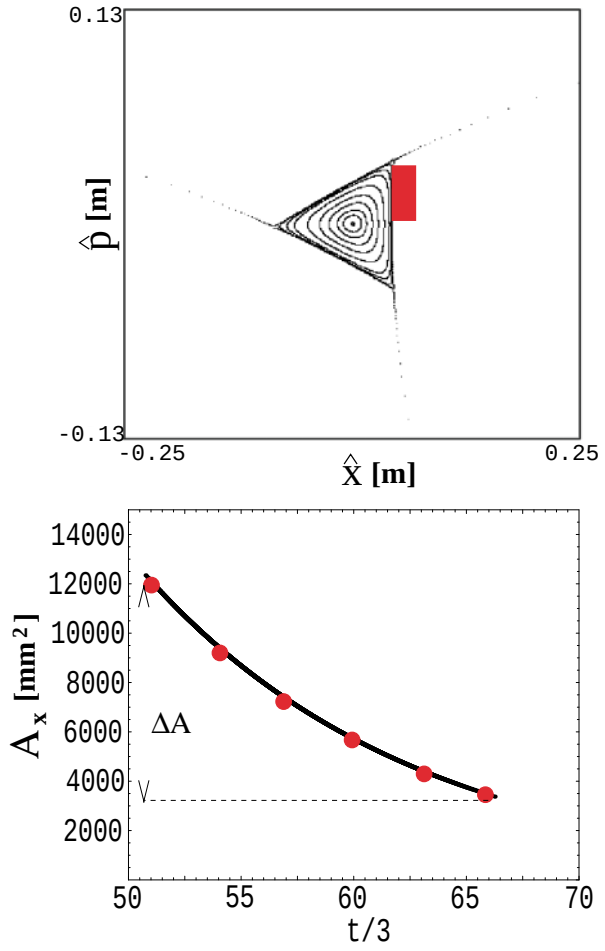

FIG. 6. (Color) Area and emittance of the extracted beam $A_x = \pi\epsilon_x$ versus extraction time during the extraction of the red stripe of particles on the top frame.

outer edges allows one to plot the shape of the emittance of the extracted beam versus time, as shown in Fig. 6. The fluctuations of the dimension of the focal spot (which depends on the transverse dimension of the extracted beam) increase with the amplitude $\Delta\epsilon$ of the emittance decrease.

(ii) Dynamic case.—When the parameters of the extraction (such as the machine tune) are changing in time slowly enough compared to the average extraction time one can consider the extraction process instantaneous and, after computing the initial coordinates $(X_0(t), P_0(t))$ of the destabilized particles according to the particular extraction scheme, use (11) to evaluate $\pi\epsilon(t) = X_0(t)P_0(t)\sigma(X_0(t)P_0(t))$.

The analysis of extraction times and emittances using the hyperbolic normal forms has not yet been discussed in the presence of space charge. This is possible provided that we determine the hyperbolic fixed point of period 3 and construct a polynomial expansion of the third iterate of the map around one of them.

IV. EXTENSION TO THE CASE OF AN INTENSE BEAM

A. Frequency analysis

To generalize the technique described in Sec. III one must take into account the shift in the position of the fixed points due to space charge. In this section we first illustrate the nonlinear effects of space charge on the transverse dynamics of the model by studying the nonlinear tune behavior.

The numerical tracking of the orbits has been carried out by transfer maps. To obtain the one turn map of the system one must break the action of space charge, continuous over the ring, into a certain number of kicks. The order of possible resonances artificially introduced by the discretization grows with the number N of space charge kicks. The one turn map approximated with N kicks reads

$$M = \underbrace{R\left(\frac{\omega}{N}\right) \circ K_{\rm sc} \circ \cdots \circ R\left(\frac{\omega}{N}\right) \circ K_{\rm sc}} \circ K_{\rm sex}\,, \tag{13}$$

where $R(\alpha)$ is the rotation matrix of angle α and

$$K_{\rm sc} = \begin{pmatrix} \hat{x} \\ \hat{p} - \frac{\hat{\xi}\hat{a}}{N}[\frac{1}{2}V'(\frac{\hat{x}}{\hat{a}}) + \frac{\hat{x}}{\hat{a}}] \end{pmatrix},$$
$$K_{\rm sex} = \begin{pmatrix} \hat{x} \\ \hat{p} + \frac{\hat{K}_2}{2}\hat{x}^2 \end{pmatrix}. \tag{14}$$

Fourier analyzing the iterates of this map for different initial conditions of increasing emittance, we have computed the nonlinear tune as a function of the emittance.

Being continuously distributed around the ring, the space charge cannot excite any resonance in a flat beam. The nonlinear tune increases steadily with the distance from the origin, reaching the bare tune $\omega_0/2\pi$ as $|x| \to \infty$. The dependence of the nonlinear frequency $\Omega_{\rm sc}$ on the orbit emittance ϵ for a generic charge distribution can be analytically described very accurately by canonical perturbation theory (see [3] for the computation for a Gaussian charge distribution). For the chosen charge distribution, letting $J = \frac{1}{2}(\hat{x}^2 + \hat{p}^2)$ be the action, we get

$$\Omega_{\rm sc} = \omega + \frac{\hat{\xi}}{2}\left[1 - \frac{2}{\sqrt{1 + 2J/\hat{a}^2}\,(1 + \sqrt{1 + 2J/\hat{a}^2})}\right], \tag{15}$$

which is plotted in Fig. 7.

When a thin sextupole is present, as in the case of slow extraction, and the linear tune approaches a resonant value, the perturbative calculations can be performed by using the resonant normal forms.

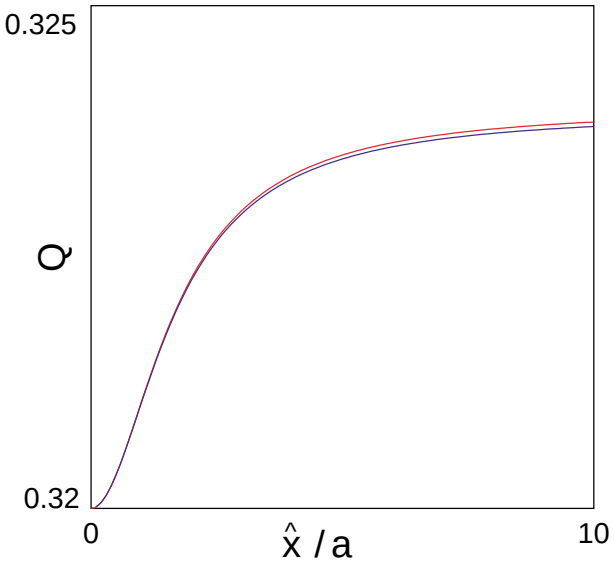

FIG. 7. (Color) Nonlinear tune ($Q = \Omega/2\pi$) analytically computed (blue line), by canonical nonresonant perturbation theory, as a function of $\hat{x}/a$ with $\hat{p} = 0$ ($2_J = \hat{x}^2$) for $\hat{\xi} = 0.05$ and linear frequency $\omega = 0.32 \times 2\pi$. The result is compared with the tune obtained by fast-Fourier transform (FFT) from tracking (red line).

1. Pure sextupole

In the case of a pure sextupole, ω and the bare machine frequency ω_0 coincide. When $\omega > 2\pi/3$ the nonlinear frequency Ω_{sex} decreases monotonically until it reaches the resonant value. On the contrary, when $\omega < 2\pi/3$, Ω_{sex} increases up to $2\pi/3$. In both cases, near the resonance the sextupole pushes Ω_{sex} toward $2\pi/3$, as can be seen with nonresonant normal form analysis [4], that gives as a first-order estimate of the nonlinear frequency

$$\Omega_{\text{sex}} = \omega - \frac{1}{16}\left(\frac{\hat{K}_2}{2}\right)^2\left[3\cot\left(\frac{\omega}{2}\right) + \cot\left(\frac{3\omega}{2}\right)\right]\epsilon\,. \tag{16}$$

If ω is close to $2\pi/3$ the coefficient of the emittance $\epsilon = \hat{x}^2 + \hat{p}^2$ is negative for $\omega > 2\pi/3$ and positive for $\omega < 2\pi/3$. As a consequence, when ϵ increases Ω_{sex} reaches the value $2\pi/3$, according to Eq. (16), if ω is above or below $2\pi/3$. When $\omega/2\pi$ is close to 0.32 three islands appear.

2. Sextupole + space charge

When ω is close to $2\pi/3$ the dependence of the dynamic aperture on the space charge intensity $\hat{\xi}$ is easily described. The frequency Ω in this case may be approximated by the linear frequency plus the sum of the space charge frequency shift $\Omega_{\text{sc}} - \omega$ given by Eq. (13) and the sextupole frequency shift $\Omega_{\text{sex}} - \omega$ given by Eq. (14). If $\omega < 2\pi/3$ the sextupole and space charge frequency shifts are both positive and the frequency $\Omega \simeq \omega + (\Omega_{\text{sex}} - \omega) + (\Omega_{\text{sc}} - \omega)$ increases with ϵ; the resonance is crossed for

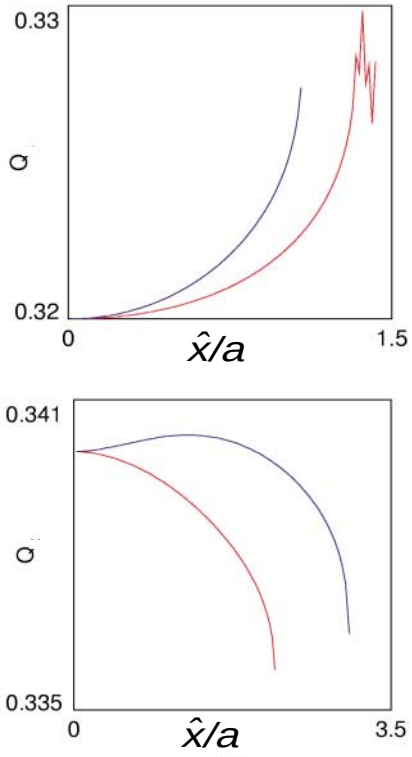

FIG. 8. (Color) Nonlinear tune $Q = \Omega/2\pi$ for a pure sextupole (red line) and a sextupole + space charge (blue line). (Top) $\omega' = 0.32 \times 2\pi$, $a\hat{K}_2' = 0.3$, $\hat{\xi} = 0.05$. (Bottom) $\omega' = 0.34 \times 2\pi$, $a\hat{K}_2' = 0.14$, $\hat{\xi} = 0.05$. The horizontal coordinate is the linearly normalized coordinate divided by the core radius a. To compare these values with a lattice such as SIS we must add the integer part to the linear tune so that $\omega = 4.32 \times 2\pi$ ($n = 13$); for $a = 25$ mm we have $\hat{K}_2 = \hat{K}_2'/\sqrt{n} = 3.3\ \text{m}^{-1}$.

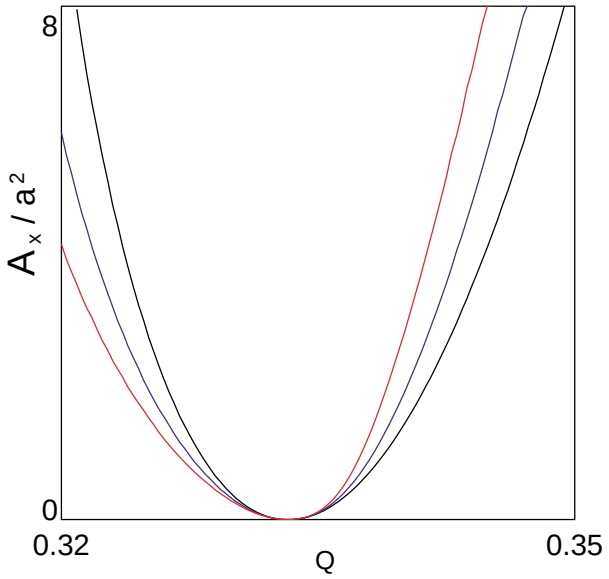

FIG. 9. (Color) Plot of the area of the stable region $A_x = \pi\epsilon_x$ normalized to a^2, as a function of the linear tune $Q = \omega/2\pi$ for $a\hat{K}_2' = 0.3$ and different values of the space charge intensity. Black line, $\hat{\xi} = 0$; blue line, $\hat{\xi} = 0.05$; red line, $\hat{\xi} = 0.1$.

a value of the emittance which decreases with $\hat{\xi}$ (see top frame of Fig. 8). If $\omega > 2\pi/3$ the sextupole frequency shift becomes negative and the frequency Ω may reach a maximum before decreasing; the resonance is crossed for a value of the emittance which increases with $\hat{\xi}$ (see bottom frame of Fig. 8). Both the increase of the dynamic aperture with $\hat{\xi}$ before $2\pi/3$ and its decrease below this value can be seen in Fig. 9, where the emittance of the stable area is plotted as a function of the bare linear tune $Q_0 = \omega_0/(2\pi)$ for increasing beam currents.

B. Elliptic interpolating Hamiltonian

To evaluate semianalytically the new position of the hyperbolic fixed points we evaluate the elliptic normal forms starting from a polynomial expansion of the one turn map M at the origin. In the normal coordinates the orbits of M can be interpolated by the orbits of a Hamiltonian $\mathcal{H}$ invariant under continuous rotations (nonresonant normal form) or under discrete rotations of $2\pi/3$ (resonant normal form). This Hamiltonian captures the relevant dynamical features of the map.

To calculate the normal form of the proposed Hamiltonian one must, first, replace the space charge force by a polynomial approximation. A polynomial of degree 3 or 5 gives a good approximation up to one-half the core radius or core radius itself; see Fig. 10. Next, calculate a polynomial map by composing N times a rotation of ω/N, with space charge kicks and one sextupolar kick at the end [see Eqs. (13) and (14)]. Finally, compute, by using a computer program such as ARES [5] or BIRKHOFF [6], the elliptic normal form and its interpolating Hamiltonian (the polynomial map is truncated at degree $2n - 1$ in order to compute their order n normal form).

In Figs. 11 and 12 we show that the phase portraits obtained with the space charge force F given by Eq. (3) and with a polynomial approximation of degree 5 are very similar up to the hyperbolic fixed points. Moreover, the top frame of Fig. 13 shows that the nonlinear tunes (computed by Fourier analyzing the orbit obtained from tracking) corresponding to F and its approximation of degree 5 are very close up to the dynamic aperture (end point of the red line).[1] As a consequence, polynomial expansions of the space charge force beyond fifth order are not needed.

[1]The approximating polynomial has a slightly bigger dynamic aperture than the original map for the condition of Fig. 13, as one can see in the bottom phase space portrait of Fig. 12. Hence the nonlinear tunes, defined for every stable orbit, extend a bit further. Such information is, however, uninteresting because, wishing to locate the hyperbolic fixed points, we ask the approximating map to reproduce the system dynamics just up to that point.

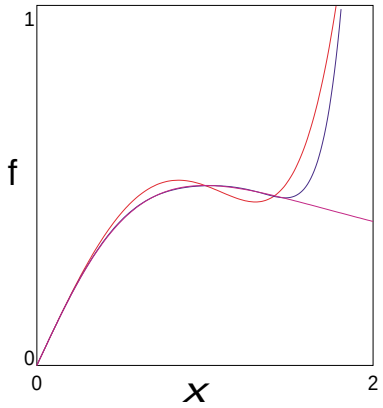

FIG. 10. (Color) Polynomial approximation of the space charge force $F(x) = \zeta a^{-1} f(x/a)$, where $f(x) = x/(1 + x^2)$. Function $f(x)$ (violet line), approximation of order 5 $f_5(x) = x - \frac{2}{3}x^3 + \frac{1}{6}x^5$ (red line), approximation of order 9 $f_9(x) = x - 0.9268x^3 + 0.6313x^5 - 0.2430x^7 + 0.0378x^9$ (blue line) obtained by minimizing the L^2 norm in $[0, 1.5]$.

The order n of the normal form ($\mathcal{H}$ is a polynomial of degree $2n$) is chosen by demanding that the frequency (Ω is a polynomial of degree $2n - 2$) reaches a given accuracy. To obtain the nonlinear frequency Ω we write the interpolating Hamiltonian $\mathcal{H}$ as a function of the action and angle variables J, θ, where $\hat{x} = \sqrt{2J}\cos\theta$, $\hat{p} = -\sqrt{2J}\sin\theta$, and evaluate

$$\frac{1}{\Omega(J)} = \frac{1}{2\pi}\int_0^{2\pi}\left[\frac{\partial\mathcal{H}(J,\theta)}{\partial J}\right]^{-1} d\theta\,, \qquad (17)$$

where $J = J(\theta, E)$ is implicitly defined by $\mathcal{H}(J, \theta) = E \equiv \mathcal{H}(\theta_0, J_0)$. In the bottom graph of Fig. 13 the nonlinear tune calculated via (17) is compared with the results of a Fourier analysis of the orbit of the polynomial map. At second order (highest power of J is 2) the interpolating Hamiltonian has a simple analytical expression, which allows one to compute its critical points and an approximation to the area of stable orbits. This estimate allows one to recover an approximate self-consistency of the model. Again we approximate the space charge F defined by Eq. (3) with a polynomial of degree 5 given by $F_{\text{app}} = \frac{\xi}{a}(\frac{x}{a} + \alpha\frac{x^3}{a^3} + \beta\frac{x^5}{a^5})$. The coefficients that minimize the distance (in the L^2 norm) from the exact F for $x \in [0, 1.5a]$ are $\alpha = -2/3$ and $\beta = 1/6$. In the appendix the procedure to compute a polynomial approximation of the one turn map, in the presence of a space charge force continuously acting along the ring, is outlined. The corresponding interpolating Hamiltonian reads

$$\mathcal{H} = \eta J - \frac{\hat{K}_2}{16}\frac{\eta}{\sin(3\eta/2)}(2J)^{3/2}\cos\left(3\theta + \frac{3\eta}{2}\right) + J^2 \times\left[\frac{3\hat{K}_2^2}{128}\eta\left(1 + \cot^2\frac{3\eta}{2} - \frac{2}{3\eta}\cot\frac{3\eta}{2}\right) - \frac{3\hat{K}_2^2}{64}\cot\frac{\omega}{2} - \frac{3}{8}\hat{\alpha}\right], \qquad (18)$$

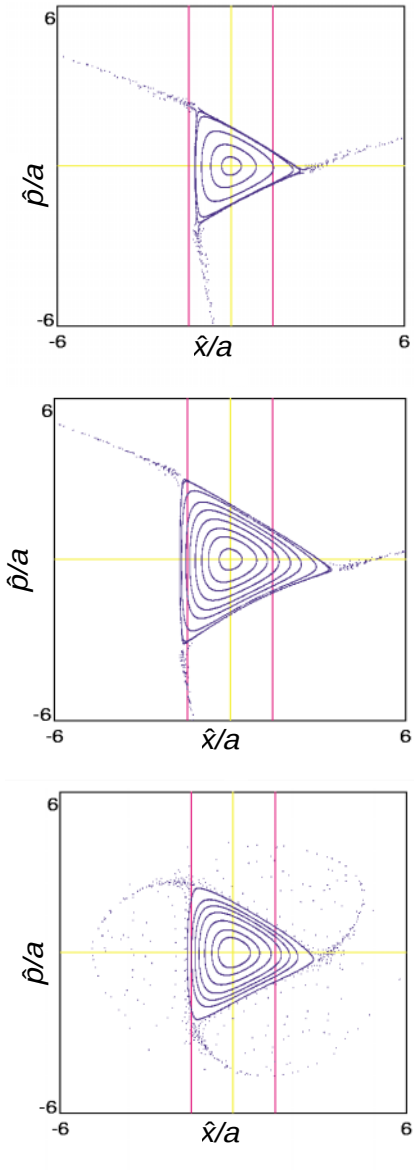

FIG. 11. (Color) (Top) Pure sextupole with $\omega' = 0.34 \times 2\pi$ and $a\hat{K}_2' = 0.14$. (Center) Exact sextupole + space charge with $\omega' = 0.34 \times 2\pi$, $a\hat{K}_2' = 0.14$, and $\hat{\xi} = 0.05$. (Bottom) Exact sextupole + space charge where the space charge force $F(x)$ is replaced with a polynomial approximation of degree 5. The phase plots are in the coordinates $\hat{x}, \hat{p}$ normalized to the core radius a. The dynamic aperture is comparable to the normalized core radius $\hat{x}_{\mathrm{dyn}} \simeq \hat{a} \simeq 1.4a$. To compare these values with a lattice such as SIS, we must add the integer part to the tune $\omega = 4.34 \times 2\pi$, and for $a = 25$ mm we have $\hat{K}_2 = \hat{K}_2'/\sqrt{n} = 1.5\ \mathrm{m}^{-1}$. Purple vertical lines $\hat{x} = \pm\hat{a} \simeq \pm 1.4a$.

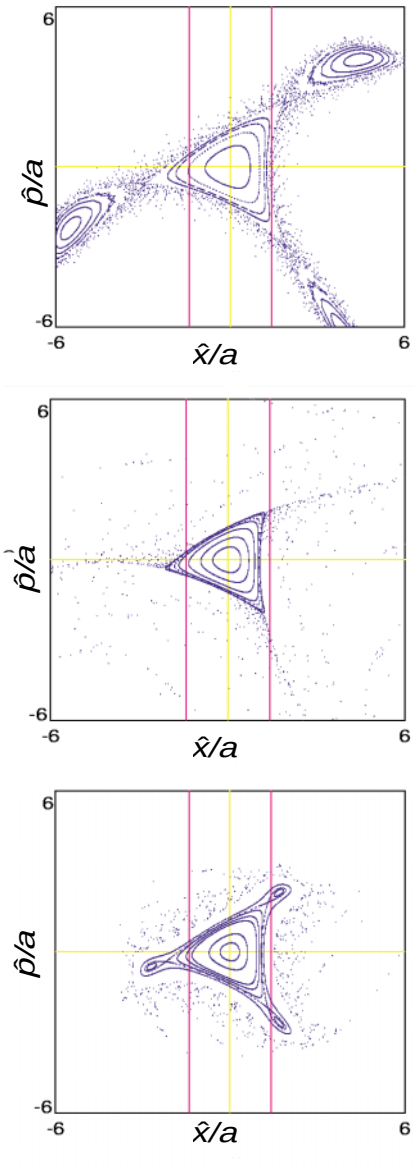

FIG. 12. (Color (Top) Pure sextupole with $\omega' = 0.32 \times 2\pi$ and $a\hat{K}_2' = 0.3$. (Center) Exact sextupole + space charge with $\omega' = 0.32 \times 2\pi$, $a\hat{K}_2' = 0.3$, and $\hat{\xi} = 0.05$. (Bottom) Exact sextupole + space charge where the space charge force $F(x)$ is replaced with a polynomial approximation of degree 5. The phase plots are in the coordinates $\hat{x}, \hat{p}$ normalized to the core radius a. The dynamic aperture is comparable to the normalized core radius $\hat{x}_{\mathrm{dyn}} \simeq \hat{a} \simeq 1.4a$. To compare these values with a lattice such as SIS, we must add the integer part to the tune $\omega = 4.32 \times 2\pi$, and for $a = 25$ mm we have $\hat{K}_2 = \hat{K}_2'/\sqrt{n} = 3.3\ \mathrm{m}^{-1}$. Purple vertical lines $\hat{x} = \pm\hat{a} \simeq \pm 1.4a$.

where η is the distance of the linear frequency from the resonance: $\omega = \Omega(0) = 2\pi(m + \frac{1}{3}) + \eta$ and $\hat{\alpha} = \alpha\hat{\xi}/\hat{a}^2 = -(2\hat{\xi}/3\hat{a}^2)$ is the coefficient of the third-order contribution of the space charge kick in Courant-Snyder coordinates. We remark that $\mathcal{H}$ for $\hat{\alpha} = 0$ and $\hat{K}_2 = 2$ is the interpolating Hamiltonian of the Hénon map.

This Hamiltonian allows one to compute a correction in the position of the fixed points which depends on the coefficient $\hat{\alpha}$ of the first nonlinear correction of the space charge force. [At the previous perturbative order, that is, taking into account terms just up to $j^{3/2}$, the nonlinear contributions of space charge do not enter the Hamiltonian

and the stable area reads $A_x = 16\sin^2(3\eta/2)\frac{1}{\sqrt{3}}(2/\hat{K}_2)^2$. For $\eta \to 0$, the dynamic aperture, given by the half height of the equilateral triangle of area A_x is $\hat{x}_{\rm dyn} = 6|\eta|/\hat{K}_2$. The ratio A_x/a^2 depends on the dimensionless parameter $a\hat{K}_2$.] If ω is sufficiently near to $2\pi/3t$ so that no stable chain of three islands is present, we can approximate the stable region as a triangle and compute its area,

$$A_x(\eta,\hat{K}_2,\hat{\xi},\hat{a}) = 3\sqrt{3}\,\eta\left(\frac{2}{\hat{K}_2}\right)^2 \times \frac{\left[\frac{3\sqrt{\eta}}{\sin(\frac{3\eta}{2})} - \sqrt{-128\frac{\hat{\xi}}{\hat{a}^2}(\frac{2}{\hat{K}_2})^2 - 24\eta + 16\cot(\frac{3\eta}{2}) + \frac{9\eta}{\sin^2(\frac{3\eta}{2})} - 24\eta\cot(\frac{3\eta}{2})^2 + 48\cot(\frac{2\pi+3\eta}{6})}\right]^2}{[-16\frac{\hat{\xi}}{\hat{a}^2}(\frac{2}{\hat{K}_2})^2 - 3\eta - 3\eta\cot(\frac{3\eta}{2})^2 + 2\cot(\frac{3\eta}{2}) + 6\cot(\frac{2\pi+3\eta}{6})]^2}. \tag{19}$$

In Fig. 14 the emittance of the stable area numerically computed is compared with its analytical estimate.

The condition $A_x(\eta,\hat{K}_2,\hat{\xi},\hat{a}) = \pi\hat{a}^2$ allows one to impose that the radius of the charge distribution is equal to the radius of the stable area in phase space and determines $\hat{a} = \hat{a}(\eta,\hat{K}_2,\hat{\xi})$.

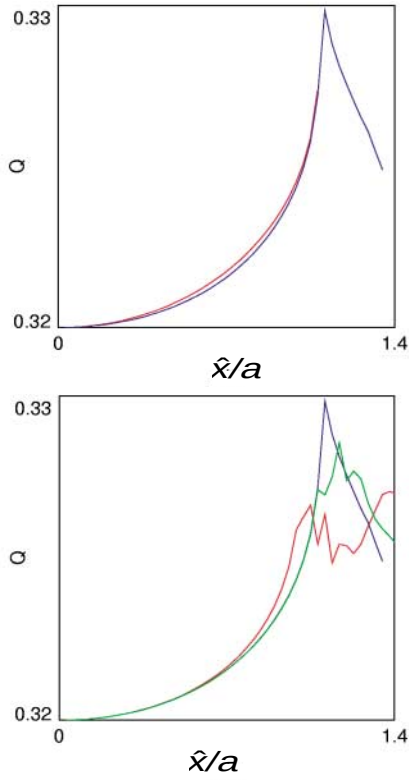

FIG. 13. (Color) (Top) Comparison of the nonlinear tune $Q = \Omega/2\pi$ (computed with a FFT) for the map M (red line) with $\hat{\xi} = 0.05$, $a\hat{K}_2' = 0.3$, $\omega' = 0.32 \times 2\pi$, and the map $\overline{M}$ with a space charge force approximated by a polynomial of order 5 (blue line). (Bottom) Comparison of nonlinear tune (computed with a FFT) for the map $\overline{M}$ (blue line) with the tune obtained from resonant normal form approximations of order 3 (red line) and 4 (green line). The horizontal coordinate is the linearly normalized coordinate $\hat{x}$ divided by the core radius a.

After computing the new fixed point position one can use the technique illustrated in Sec. III in order to compute the extraction times. An accurate calculation requires a polynomial expansion of the complete one turn map (sextupole + space charge) at the fixed point. For low values of $\hat{\xi}$, however, it is sufficient to take into account just the linear effect of space charge, and one can directly apply the results of Sec. III provided that the shifted linear frequency $\omega = \omega_0 - 2\pi\Delta Q_{\rm sc}$ is used. For higher space charge the change of the stable area may be taken into account by introducing an equivalent sextupole with gradient $\hat{K}_{2,\rm eq}$. This is determined by imposing that the stable area for such a sextupole without space charge is the same as for the sextupole with gradient $\hat{K}_2$ with space charge. Using (19) this condition reads

$$A_x(\eta,\hat{K}_{2\rm eq},0,\hat{a}) = A_x(\eta,\hat{K}_2,\hat{\xi},\hat{a})\,. \tag{20}$$

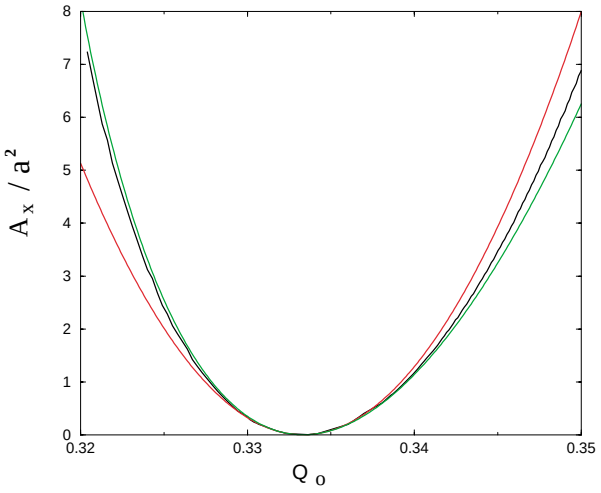

FIG. 14. (Color) Numerical values (black line) and analytical estimates, obtained from the Hamiltonian $\mathcal{H}$ at order $J^{3/2}$ (red line) and order J^2 (green line), of the area $A_x = \pi\epsilon_x$ of the stable region, normalized to a^2, for a pure sextupole with $a\hat{K}_2 = 0.33$. The area is plotted as a function of the linear tune $Q_0 = \omega_0/2\pi$.

V. CONCLUSIONS

A method based on hyperbolic normal forms is proposed to obtain semianalytical estimates of the extraction time and of the extracted emittance in a resonant (slow) extraction process. A good agreement with tracking is found. The dynamical and geometrical features of the extraction process emerge very neatly in the normal coordinates plane.

The space charge changes the tune and the location of the unstable periodic points. The resonant normal forms allow one to describe the changes of the tune and of the area of the stable region, once a polynomial approximation to the space charge force is introduced. Moreover, an approximate self-consistency can be imposed by equating the stable area to the area of the core cross section. The results are qualitatively correct at the lowest order, very close to tracking when the order is increased.

A simple description of the extraction process, valid for moderate space charge intensities, consists of using a thin sextupole Hamiltonian with an effective strength such that the stable area is the same as for the model with space charge.

APPENDIX: COMPUTATION OF THE POLYNOMIAL ONE TURN MAP FOR A SEXTUPOLE AND SPACE CHARGE

We define $M_{\mathrm{sc+sex}}$ the one turn map on the normalized lattice (of unit length) with respect to the linearly normalized coordinates $(\hat{x},\hat{p})$. This is the result of the space charge map and the final sextupoles kick.

$$M_{\mathrm{tot}} = M_{\mathrm{sc}} \circ M_{\mathrm{sex}}\,, \tag{A1}$$

where the space charge map is the limit of n space charge kicks $M_{\mathrm{sc}}(\frac{1}{n})$ acting on arcs of length $1/n$ according to $M_{\mathrm{sc}} = \lim_{n\to\infty} M_{\mathrm{sc}}^{\circ n}(\frac{1}{n})$.

The one turn map in the linearly normalized coordinates $(\hat{x},\hat{p})$ reads

$$M_{\mathrm{sc+sex}}(z) = M_{\mathrm{sc}} \circ \left[z - i\,\frac{\hat{K}_2}{8}\,(z+z^*)^2 \right], \tag{A2}$$

where $z = \hat{x} - i\hat{p}$. The space charge map on an arc of length $1/n$ is given by

$$M_{\mathrm{sc}}\left(\frac{1}{n}\right) = e^{i\delta}\left[z - i\,\frac{\hat{\alpha}}{8n}\,(z+z^*)^3 \right], \tag{A3}$$

where $\delta = \omega/n$, and the nonlinear space charge coefficient is defined as previously by $\hat{\alpha} = \alpha\hat{\xi}/\hat{a}^2 = -\frac{2}{3}\hat{\xi}/\hat{a}^2$. To evaluate M_{sc} we conjugate $M_{\mathrm{sc}}(\frac{1}{n})$ to its nonresonant normal form according to

$$M_{\mathrm{sc}}\left(\frac{1}{n}\right) = \Phi \circ U \circ \Phi^{-1},$$

$$U = z\exp\left(i\delta - i\,\frac{3}{8}\,\frac{\hat{\alpha}}{n}\,zz^* \right),$$

where up to order 3 we have $\Phi = z + \Phi_{30}z^3 + \Phi_{21}z^2z^* + \Phi_{12}zz^{*2} + \Phi_{03}z^{*3}$. Imposing the area preserving condition, the coefficients are determined according to

$$\Phi_{30} = -\frac{i\alpha}{8n}\,\frac{e^{i\delta}}{e^{3i\delta} - e^{i\delta}}\,,$$

$$\Phi_{12} = 0\,,$$

$$\Phi_{21} = -\frac{3i\alpha}{8n}\,\frac{e^{i\delta}}{e^{-i\delta} - e^{i\delta}}\,,$$

$$\Phi_{03} = -\frac{i\alpha}{8n}\,\frac{e^{i\delta}}{e^{-3i\delta} - e^{i\delta}}\,,$$

The iterate of order n is determined by $M_{\mathrm{sc}}^{\circ n}(\frac{1}{n}) = \Phi \circ U^{\circ n} \circ \Phi^{-1}$, and expanding up to order 3 we find

$$M_{\mathrm{sc}}^{\circ n}\left(\frac{1}{n}\right) = e^{in\delta}z - i\,\frac{\hat{\alpha}}{8n}\,e^{i\delta}\left[\frac{e^{i3n\delta} - e^{in\delta}}{e^{i3\delta} - e^{i\delta}}\,z^3 + 3ne^{i(n-1)\delta}z^2z^* + \frac{e^{-in\delta} - e^{in\delta}}{e^{-i\delta} - e^{i\delta}}\,3zz^{*2} + \frac{e^{-i3n\delta} - e^{in\delta}}{e^{-i3\delta} - e^{i\delta}}\,z^{*3} + \cdots \right]. \tag{A4}$$

Taking the $n \to \infty$ limit and composing with the sextupole kick, the final one turn map reads

$$M_{\mathrm{tot}} = e^{i\omega}\left[z - i\,\frac{\hat{K}_2}{8}\,(z+z^*)^2 - i\,\frac{\hat{\alpha}}{8}\,\frac{1}{\omega}\left(\frac{z^3}{\cot\omega - i} + 3\omega z^2z^* + \frac{3zz^{*2}}{\cot\omega + i} + \frac{z^{*3}}{\cot 2\omega + i} \right) + \cdots \right]. \tag{A5}$$

[1] Accelerator Complex Study Group, CERN-PS division Internal Note No. PS 99-010, 1999, http://atlasinfo.cern.ch/CERN/Divisions/PS/Reports/R1999/1999.html.

[2] G. L. Da Silva, A. M. Ozoiro De Almeida, and R. Douady, Physica (Amsterdam) **29D**, 181–190 (1987).

[3] A. W. Chao, in *Proceedings of the Conference on Nonlinear Aspects of Particle Accelerators, Sardinia, 1995* (CERN, Geneva, 1994).

[4] A. Bazzani, E. Todesco, G. Servizi, and G. Turchetti, CERN Yellow Report No. 94-02, 1994.

[5] G. Servizi and G. Turchetti, Comput. Phys. Commun. **32**, 201–207 (1984).

[6] A. Bazzani, M. Giovannozzi, and E. Todesco, Comput. Phys. Commun. **86**, 199 (1995).